Bioorganic & Medicinal Chemistry 18 (2010) 2049–2059

Contents lists available at ScienceDirect

Bioorganic & Medicinal Chemistry

journal homepage: www.elsevier.com/locate/bmc

Interaction of (benzylidene-hydrazono)-1,4-dihydropyridines with β-amyloid, acetylcholine, and butyrylcholine esterases

Vildan Alptüzün [a], Michaela Prinz [b], Verena Hörr [b], Josef Scheiber [b,†], Krzysztof Radacki [c], Adyary Fallarero [d], Pia Vuorela [d], Bernd Engels [e], Holger Braunschweig [c], Ercin Erciyas [a], Ulrike Holzgrabe [b,*]

[a] Faculty of Pharmacy, Ege-University, Bornova-Izmir, Turkey
[b] Institute of Pharmacy and Food Chemistry, University of Würzburg, Am Hubland, 97074 Würzburg, Germany
[c] Institute of Inorganic Chemistry, University of Würzburg, Am Hubland, 97074 Würzburg, Germany
[d] Division of Pharmacy, Faculty of Mathematics and Natural Sciences Åbo Akademi University BioCity, Artillerigatan 6A, FI-20520 Turku, Finland
[e] Institute of Organic Chemistry, University of Würzburg, Am Hubland, Würzburg, Germany

ARTICLE INFO

Article history:
Received 26 October 2009
Revised 22 December 2009
Accepted 2 January 2010
Available online 15 January 2010

Keywords:
AChE inhibitors
β-Amyloid plaques
(Benzylidene-hydrazono)-1,4-dihydropyridines

ABSTRACT

Approved drugs for the treatment of Alzheimer's disease belong to the group of inhibitors of the acetylcholinesterase (AChE) and NMDA receptor inhibitors. However none of the drugs is able to combat or reverse the progression of the disease. Thus, the recently reported promising multitarget-directed molecule approach was applied here. Using the lead compound **DUO3**, which was found to be a potent inhibitor of the AChE and butyrylcholinesterase (BuChE) as well as an inhibitor of the formation of the amyloid (Aβ) plaque, new non-permanently positively charged derivatives were synthesized and biologically characterized. In contrast to **DUO3** the new bisphenyl-substituted pyridinylidene hydrazones **5** are appropriate to cross the blood–brain barrier due to their pK_a values and lipophilicity, and to inhibit both the AChE and BuChE. More important some of the pyridinylidene hydrazones inhibit the Aβ fibril formation completely and destruct the already formed fibrils significantly.

1. Introduction

Alzheimer's disease (AD) is a progressive neurodegenerative disease characterized by a loss of cognitive function and behavioral abnormalities. Immense efforts have been made to develop efficient strategies for the treatment of AD because of its greatly increased prevalence. According to predictions the number of AD cases in the western world will double every 20 years and even triple in India and China with 29 million people in 2020, mostly owed to increased human longevity.[1]

Due to the multifactorial nature of involved processes, recently nicely summarized in Ref. 2, for example, protein misfolding and aggregation, intracellular oxidative stress and free radical formation, elevated levels of trace metals, mitochondrial dysfunction, and phosphorylation impairment, several attempts have been conducted to overcome the development of the progressive and eventually fatal neurodegenerative disease. Among others the most important, current treatment strategies are the approved cholinesterase inhibitors (see below) and NMDA (*N*-methyl-D-aspartate) receptor antagonists, that is, memantine, and substances in clinical trials, for example, amyloid-β (Aβ) aggregation inhibitors, antioxidants, γ-secretase modulators, peroxisome proliferator-activated receptors (PPAR) γ agonists, H3 antagonists, and HMG-CoA reductase inhibitors.[3]

Among different neurotransmitter deficits occurring in AD, loss of cholinergic neurons and resulting deficit of neurotransmitter acetylcholine (ACh), and presynaptic M_2 muscarinic and nicotinic receptors have been found.[4] These findings led to the *cholinergic hypothesis* postulating that many of the cognitive, functional, and behavioral symptoms experienced by AD patients are a consequence of deficient cholinergic neurotransmission.[5] Hence for the most part, inhibitors of acetylcholinesterase, enhancing the acetylcholine concentration in the brain, have been introduced to the market for treating mild-to-moderate AD. Well-known examples are tacrine, galanthamine, rivastigmine, and donepezil.[6] Another promising approach is the development of dual inhibitors for AChE and butyrylcholinesterase (BuChE),[7] as BuChE activity seems to correlate with AChE activity in AD and a cognitive improvement could be reached.[8,9] Recently, dimebon, originally approved as a non-selective antihistamine, was discovered to weakly inhibit the BuChE and AChE, weakly block the NMDA receptor signaling pathway and inhibit mitochondrial permeability transition pore opening. Due to neuroprotective effects observed in models for AD's and Huntington's disease, a clinical trial phase III revealed a significant improvement of the cognition of AD patients.[10] However, none of these disease-modifying anti-Alzheimer's drugs is able to

* Corresponding author. Tel.: +49 931 888 5460; fax: +49 931 888 5494.
E-mail address: u.holzgrabe@pzlc.uni-wuerzburg.de (U. Holzgrabe).
† Present address: Roche, Nonnenwald 2, Penzberg, Germany.

0968-0896/$ - see front matter © 2010 Elsevier Ltd. All rights reserved.
doi:10.1016/j.bmc.2010.01.002

combat or reverse the progression of the disease; they are only able to delay the process, emphasizing the need for more potent AD drugs to modify the disease rather than treating its symptoms only.

The deposition of Aβ in the brain is the pathological hallmark of AD and one of the potential reasons of the neuronal damage.[11] Aβ is a fragment of 37–42 amino acids excised from the transmembrane region of the amyloid precursor protein (APP) by the sequential action of β-site APP cleaving enzyme (BACE = β-secretase) and γ-secretase, eventually resulting in neurotoxicity, tau hyperphosphorylation and Aβ oligomerization, aggregation, and finally plaque formation. Consequently, inhibitors of BACE and γ-secretase are prime objectives for AD drug development.[12]

Several substances of peptidic[13] and non-peptidic origin with anti-amyloid potency were reported. Among the latter are endogenous compounds such as melatonin, in addition to rifampicin, benzofuran, benzothiazole, hydroxyindole, curcumin-derived pyrazoles and isoxazoles, and naphthylazo derivatives, phenols, classical antibiotics, for example, tetracycline as well as cyclodextrins.[14] In addition, the role of AChE is not only the hydrolysis of the neurotransmitter ACh, but also the acceleration of the aggregation of Aβ into amyloid fibrils. Responsible for this activity seems to be the peripheral anionic site (PAS) of AChE gorge.[15] Within this context, it is expected that even a peripheral site blocker prevents the Aβ peptide to interact with AChE, and, thus, inhibits the fibril formation process. Studies regarding the development of such AChE inhibitors were already reported, for example, for coumarine derivatives.[16]

In order to achieve the highest efficiency the new approach of multitarget-directed molecules introduced by Melchiorre and coworkers[17] seems to be promising. In this study we aimed to address the active site as well as the peripheral site of the AChE, the active site of the BuChE, and the Aβ in order to inhibit the formation of the amyloid fibril plaque or reverse the fibril formation. The multitarget approach might open the door to overcome the clinical problems with drugs targeting the Aβ deposition only.[18] Parts of the concept has already worked, for example, for phenserine,[19] benzofuran-based hybrid compounds,[20] and tacrine–donezepil hybrids.[21]

The group of **DUO** compounds (see Chart 1), derived from the reactivator of the poisoned AChE obidoxim, were recently found to be potent ditopic inhibitors of AChE (*Torpedo californica*) occupying both the active site and the peripheral binding site.[22] The interactions of, for example, **DUO3** found after docking include π−π stacking and cation–π contacts with amino acid residues of the anionic substrate binding site (Trp84, Phe331, and Tyr334) and the peripheral anionic binding site (Trp279). However, molecular modeling studies also revealed the compounds being too long and thus, occupying areas of the enzyme outside the catalytic gorge. Hence, **DUO3** was systematically shortened to give the most active compound **1** in this series inhibiting the AChE in the nanomolar range of concentration.[23] Both **DUO3** and correspondingly shortened molecules were able to inhibit the amyloid fibril formation[24] and thus are appropriate lead compounds for the development of multitarget-directed molecules.

Since **1** is permanently positively charged and therefore not able to pass the blood–brain barrier (BBB), the first aim of this study was to replace the pyridinium ring with a piperidine ring (compounds **2** and **4**) whose nitrogen is under physiological conditions partially protonated (necessary for AChE interaction) and partially non-protonated (transport form) due to the expected pK_a value of approximately 7 (see Chart 1).

In order to open the possibility to pass the BBB as a prodrug we followed the chemical delivery systems developed by Bodor and co-workers[25] which is based on the dihydropyridine-pyridinium-type redox conversion of a lipophilic dihydropyridine. The latter is able to pass the BBB and the cationic, lipid-insoluble pyridinium salt can perfectly interact with the AChE. Thus, as a second aim corresponding (benzylidene-hydrazono)-1,4-dihydropyridine derivatives (compound **5**, see Chart 1) were synthesized. The quaternary salt formation is also important for the rich retention of active compound within the brain to ensure therapeutically significant concentrations. The pK_a values as well as the lipophilicity (log *P*) were determined for an estimate of the possible BBB passage. The structure of the (benzylidene-hydrazono)-1,4-dihydropyridine **5a** was elucidated by means of an X-ray analysis in order to find out, whether these compounds are principally able to form π–π stacking or π–cation driven structures which would be an indication that a corresponding interaction with the amyloid is possible.[26] All compounds were subjected to Ellman's test in order to measure the inhibitory potency towards the AChE, BuChE and to the thioflavin T staining assay in order to determine the inhibition of the amyloid fibril formation as well as the fibril destruction. Additionally, the core peptide of the Aβ42 was synthesized in order to check whether this short peptide can be used for pre-screening of the inhibition of the amyloid fibril formation.

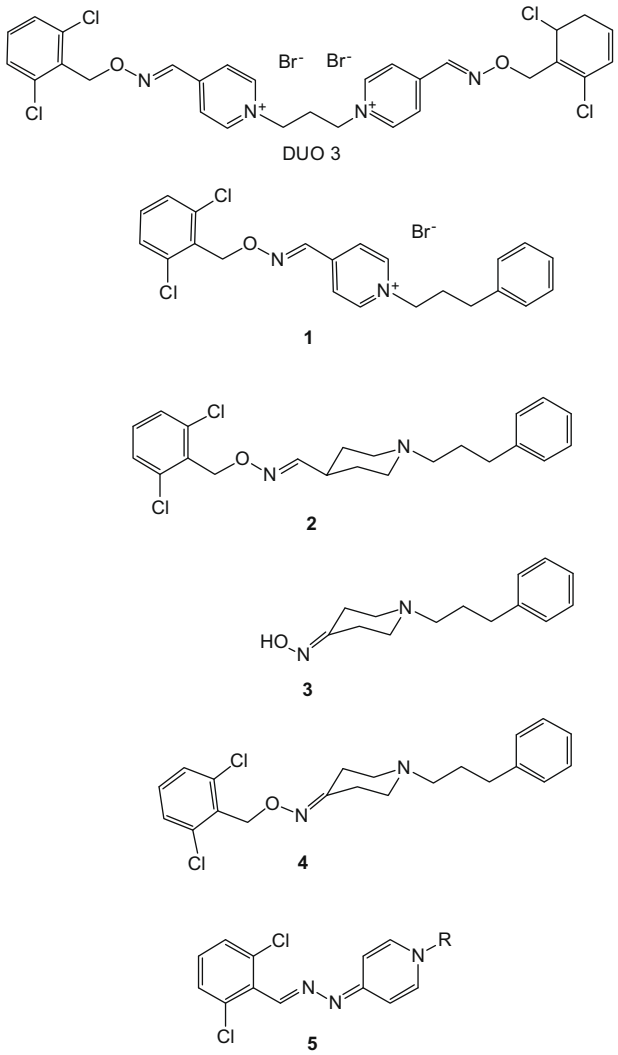

Chart 1. The lead compound **DUO3** and the derived compounds.

2. Results and discussion

2.1. Chemistry

2.1.1. Synthesis

The compounds **2**–**4** were synthesized according to Ref. 27.

Condensation of 4-hydrazinopyridine with 2,6-dichlorobenzaldehyde gave the hydrazone **6** in analogy to Douglas et al.[28] Compound **6** can be alkylated with the corresponding alkylhalogenides to give the series of (benzylidene-hydrazono)-1,4-dihydropyridine compound **5** (see Chart 2).

2.1.2. pK_a determination

In order to find out whether the newly synthesized compounds are protonated in physiological conditions (pH 7.4), and along with that positively charged, the pK_a values for compounds **2**, **4**, and **5d** were determined by means of titration using Sirius Analytical Instrument. Since the compounds were insufficiently water soluble the pK_a values were determined in water/dioxane and water/methanol mixtures.[29] Compound **2** was found to have a pK_a of approximately 7 and will be thus 50% protonated under physiological conditions which is ideal for the passage through the BBB and the π–cation interaction with Phe331 of the AChE. In comparison the corresponding piperidone oxime compound **4** is less basic (p$K_a \sim 6$) which will be advantageous for the BBB transport and disadvantageous for the AChE interaction. The (benzylidene-hydrazono)-1,4-dihydropyridine **5d** is more basic with a pK_a value of about 9 and, thus, 95% protonated at the AChE. However, the small neutral portion of **5** in equilibrium provides the possibility to pass the BBB (sink conditions).

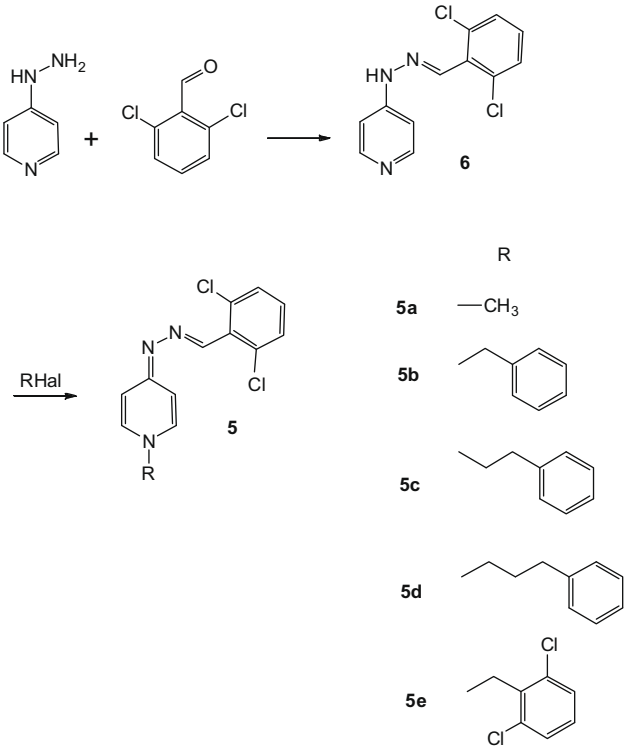

Chart 2. Synthesis pathway of compound **5**.

2.1.3. Log *P* determination

The partition coefficients were determined by means of RP HPLC using the correlation between the capacity factor and the log *P* values of reference compounds.[30] As can be seen in Table 1a, the log *P* values of compounds **3**–**5** ranged between 2.8 and 4 suggesting the possibility of the BBB passage. The log *P* of compound **4** was found to be the highest which can be explained by the low pK_a indicating a high degree of deprotonation (i.e., the neutral form) at pH 7.4. Additionally, the partition coefficients of the (benzylidene-hydrazono)-1,4-dihydropyridine **5d** and **5e** were representatively determined by the classical shake flask method in phosphate buffer at pH 5, 6, 7, and 7.4 using UV spectroscopy. The higher the pH value the more lipophilic are both compounds because according to their pK_a value the less they are protonated (see Table 1b). With a log *P* of ~3 at a pH value of 7.4 compounds **5** are sufficiently lipophilic to pass the BBB.

2.1.4. X-ray analysis

In the series of the compound **5** only the methylated compound **5a** gave crystals from methanol–water suitable for X-ray diffraction analysis. The compound **5a** crystallizes as yellow needles in the monoclinic $P2_1/n$ space group. The unit cell contains half a molecule of water. A π–π stacking between the dichlorobenzyl moieties and dihydropyridine skeleton can be seen in Figure 1 indicating that the compound may form a similar stacking with Aβ. This will be likely the same for all compound **5**.

2.2. In vitro bioassays

2.2.1. AChE/BuChE inhibition

All compounds were subjected to Ellman's test in order to evaluate their potency to inhibit the AChE (E.C. 3.1.1.7 from Electric Eel). The data are displayed in Table 1a. Interestingly, the replacement of the pyridinium ring in compound **1** with a piperidine ring resulted in a loss of activity by a factor of approximately 100 which holds true for both compounds **2** and **4**. Compound **3** missing the dichlorobenzyl group is almost inactive indicating the importance of this moiety. The potency of the hydrazone derivatives is sensitive to the substitution on the 1,4-dihydropyridine nitrogen. Compound **5a** having only a methyl group is almost inactive whereas all other compounds having an additional phenyl ring are active in the micromolar range of concentration indicating that the phenyl ring is pivotal for an interaction with the AChE. Since **5c** having a phenylethyl group has a rather low activity the phenyl ring seems not to be able to interact properly. However it has to be kept

Table 1b
pH dependent partition coefficients (log *P*) of compounds **5d** and **5e**, determined by means of the shake flask method

No.	pH			
	5	6	7	7.4
5d	0.7	0.9	1.3	3.2
5e	0.8	1.5	2.2	3.4

Table 1a
IC_{50} values, evaluated by means of Ellman's test (tacrine in this test 0.044 ± 0.004 μM) and partition coefficients of compounds **2**–**5**, determined by the RP HPLC method (the pharmacological data are the mean ± SEM, n = 3–6 experiments; IC_{50} = concentration inhibiting the AChE activity by 50%)

No.	**DUO3**	**1**	**2**	**3**	**4**	**5a**	**5b**	**5c**	**5d**	**5e**
Log *P*	0.6[50]		3.6	2.8	4.3	3.4	3.5	3.9	3.7	4.0
IC_{50} (μM) AChE	0.34 ± 0.22[47]	0.18 ± 0.007[48]	19.13 ± 1.14	277.50 ± 10.57	12.05 ± 0.08	739 ± 139.8	17.40 ± 2.56	56.70 ± 9.48	5.66 ± 0.17	6.40 ± 1.62
IC_{50} (μM) BuChE	1.83 ± 1.13	2.78 ± 1.06	Not tested	Not tested	>100	11*	8*	9*	10*	Not tested

* Due to the low activity only two experiments were performed and, therefore, no SEM are given.

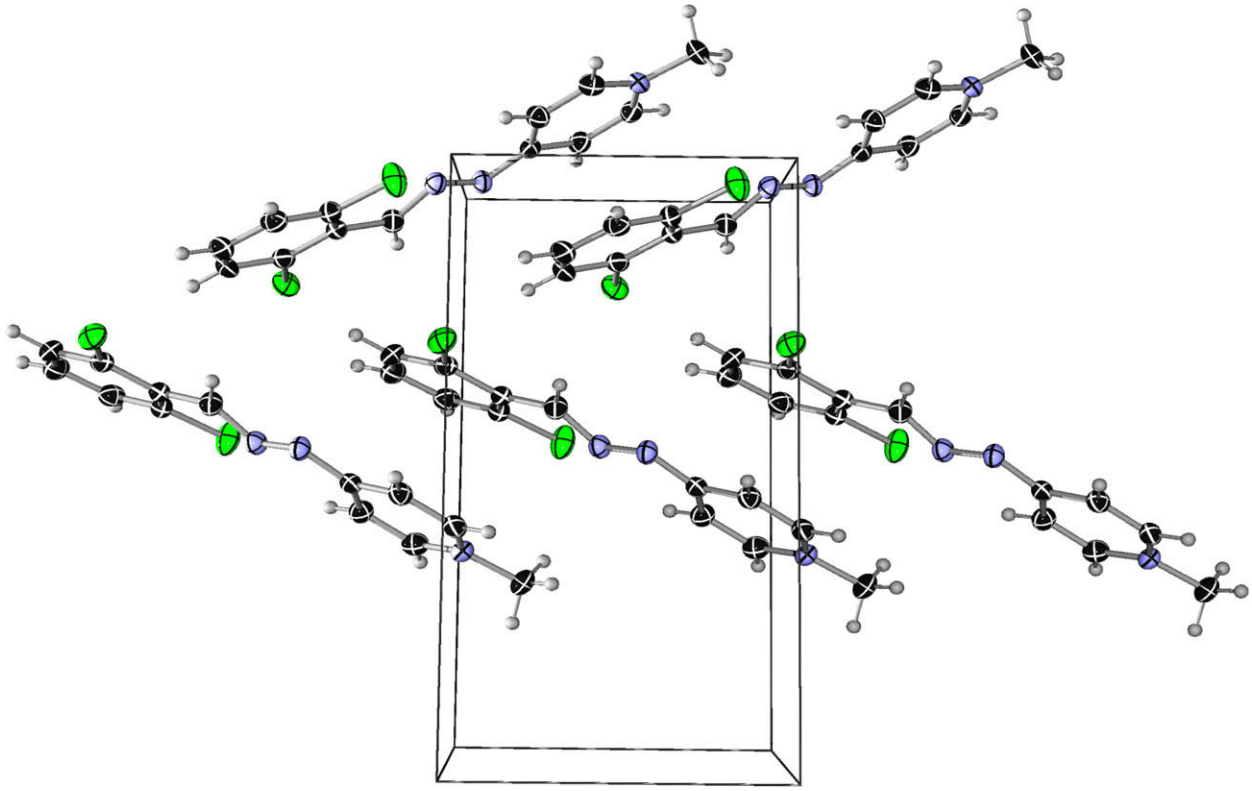

Figure 1. View along cell ***a*** axis showing π–π stacking between molecules of **5a** (water molecules omitted for clarity).

in mind, that the prodrug compound **5** might be oxidized in vivo resulting a flat, permanently positively charged pyridinium ring system as present in the highly active compound **1**.

The monitoring of the BuChE (EC 3.1.1.8, from horse serum) activity using the kinetic assay based also on Ellman's reagent and has been previously developed and validated.[11] The BuChE inhibition of the most interesting AChE inhibitors was also evaluated (cf. Table 1a). Best results showed again **DUO3** and **1**. However, all tested derivatives of compound **5** showed BuChE inhibitory activity in the low micromolar range of concentration. The activity of compound **4** was out of range, again pointing out, that an aromatic or flat unsaturated moiety in the core of the molecule is of importance.

2.2.2. Thioflavin T test

Thioflavin has been used for several decades to stain Aβ. It can visualize the block of fibril formation. The corresponding data are displayed in Figure 2. Initially, compounds **1** and **5d** having the highest AChE inhibitory activity in Ellman's test were subjected to the thioflavin T test using Aβ40 and compared to the activity of **DUO3** which was found to retard the nucleation phase of the amyloidogenesis.[49] Both compounds **1** and **5d** show similar fibril formation inhibition behavior as **DUO3** indicating that all (benzylidene-hydrazono)-1,4-dihydropyridines **5** deserve a closer inspection (see below).

Due to the high price of Aβ40 peptide, a smaller peptide featuring the same fibril formatting properties was aimed to develop. Recently a core peptide of only five highly conserved amino acids (KLVFF) was described to be responsible for fibril formation.[31] Therefore, a peptide composed of eleven amino acids and including the core sequence (HHQKLVFFAED) was synthesized and used in the thioflavin T test. The test was validated using 4-aminophenol whose IC_{50} value of blocking the Aβ oligomerization was reported to be ~90 μM.[32] Applying the core peptide revealed an IC_{50} value of

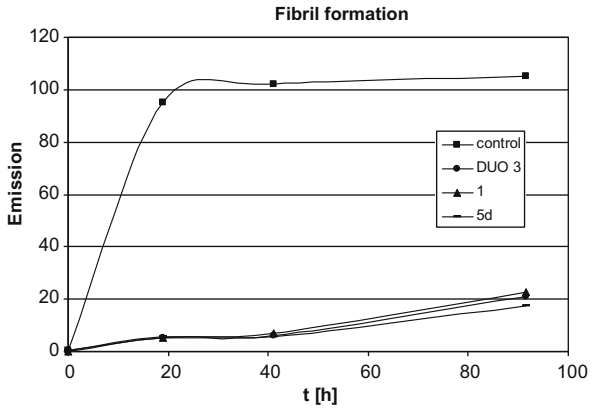

Figure 2a. Fibril inhibition of **DUO3** and its derivatives tested by ThT test with amyloid β1-40.

83 μM which is in good accordance with the aforementioned finding. Additionally, as can be seen in Figure 2b the short oligopeptide showed almost identical results concerning the fibril formation and their inhibition by the compounds **DUO3**, **1**, and **5d**. A similar approach was recently reported where a corresponding core peptide flanked with a β-sheet-promoting sequence 8(Leu-Ser)$_n$) was used.[33]

Due to the encouraging results with **DUO3**, **1**, and **5d** the test was extended to all compounds **5a–e** (see Fig. 2c). With exception of compound **5a** having no phenyl moiety attached to the pyridine nitrogen all compound show an inhibition of the fibril aggregation between 60% and 92% at a concentration of 0.5 mM. Since **5c** and **5d** having an ethyl and propyl linker between the pyridone and the phenyl ring (at the dihydropyridine nitrogen) show the highest activity, the inhibition of the fibril formation of the latter com-

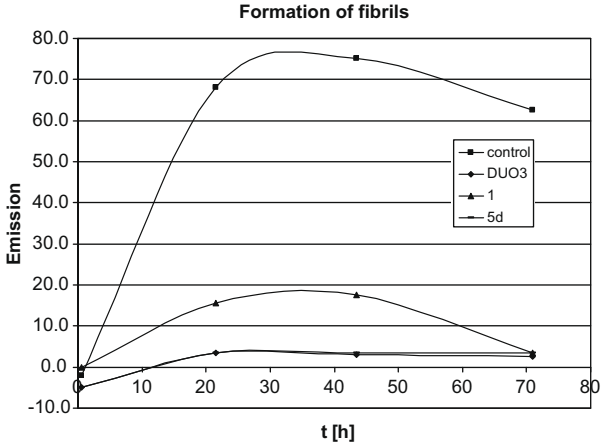

Figure 2b. Fibril inhibition of **DUO3** and its derivatives **1** and **5d** tested by ThT test with shortened peptide.

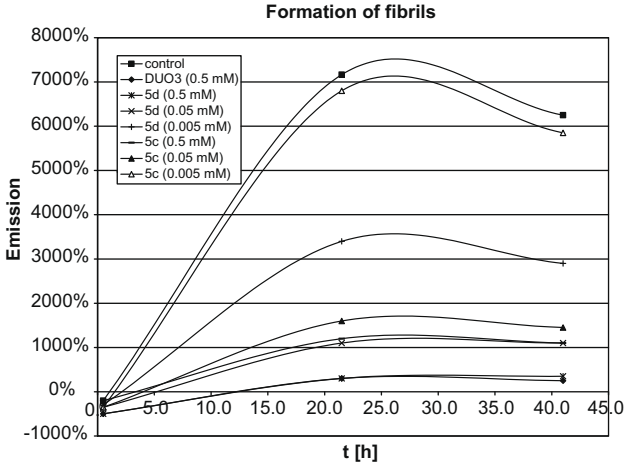

Figure 2d. Concentration-dependent fibril inhibition of 4(1*H*)-pyridinylidene hydrazones **5c** and **5d** tested by ThT test with shortened peptide.

pounds was measured concentration dependently (see Fig. 2d). Even at a concentration of 0.05 mM an inhibition of about 64% and 58% was observed for **5d** and **5c**, respectively.

Prompted by the good results, the compounds were subjected to a modified test system, where fibril destruction can be measured. Figure 2e representatively displays the concentration-dependent effect of **5d** on the fibril destruction. The destruction occurs very quickly within the first minutes as can be seen from the low starting fluorescence emission in comparison to the control. After a further small decrease within the next 5 min the emission stays constant at least until 15 h (data not shown). With exception of **5a** all other compounds show concentration-dependent similar effects (data not shown).

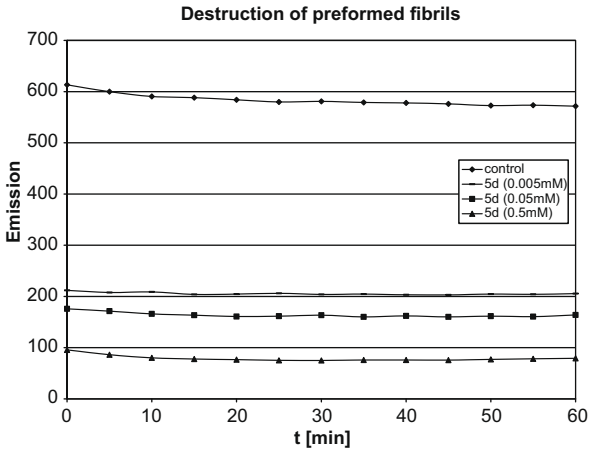

Figure 2e. Concentration-dependent fibril destruction of **5d** tested by ThT test with shortened peptide-amyloid.

2.3. Molecular modeling of the AChE interaction

The possible interactions between the compounds and AChE were determined by calculating a score that applies a measure for the strength of the interaction between the binding pocket and the structure of the ligands. To investigate possible binding modes of the compounds synthesized we performed qualitative docking experiments. This means that we are trying to elucidate possible binding modes, but we are not using the calculated docking score for the bonding strength as the latter one is known to deliver imprecise results.[34] Consequently, we used the following workflow.

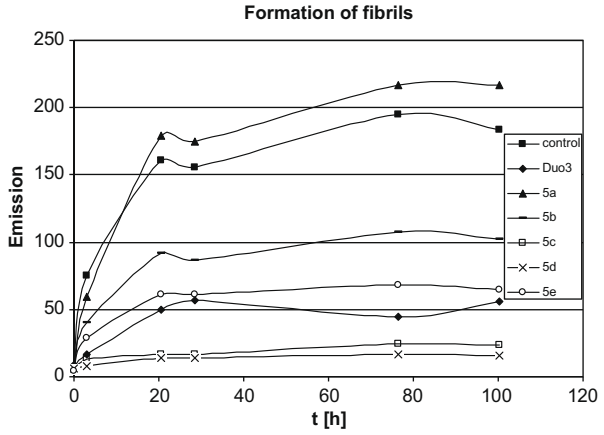

Figure 2c. Fibril inhibition of 4(1*H*)-pyridinylidene hydrazones **5a**–**e** tested by ThT test with shortened peptide.

From the pH value one can assume that the compounds are protonated only at one position. To determine the most basic protonation sites the various possibilities were computed and compared. As an initial step a set of conformers for each compound was generated using the MMFF94 force field as implemented in Macromodel.[35] The resulting structures served as starting point of subsequent DFT calculations. In these computations an aqueous solution was mimicked employing the COSMO[36] approach implemented in Turbomole.[37] For these computations the BP86 functional[38] was used in combination with basis sets of TZVP quality and the RI approximation.[39] The calculations predict that compounds **2** and **4** are firstly protonated at the amine group of the piperidine moiety. For compound **5d** the azine group was computed to be the most basic one. Based on these DFT/COSMO calculations the standard COSMO-RS[40] method implemented in COSMOTHERM program was applied to predict the acidity of the compounds. The results are in good concordance with the experimental pK_a values indicating the reliability of the predicted protonated structures (pK_a: **2** exp. = 7.1; calcd = 7.1; **4** exp. = 5.7; calcd = 6.1; **5d** exp. = 8.7; calcd = 10.6).

For docking purposes, the connection table with calculated protonation states for each compound was used as an input for a docking with Openeye FRED. Interpretation of the poses generated during docking straightforwardly represents the activities seen in

experiment (for details please refer to Section 4). We always used the top-ranking pose determined by consensus scoring as input for a detailed visual investigation which is described in the following as this is expected to provide unbiased results. As a target structure we used AChE from *T. californica* (PDB: 1EVE) as it was successfully used in previous investigations.[47] Furthermore it contains Donepezil as co-crystallized ligand, which has a structure that is somewhat related to our compounds.

Whereas the highly active compound **1** shows an excellent interaction between the dichlorobenzyl ring and Trp84, the pyridinium ring and Phe331, and the phenyl ring and Trp 279 (see Fig. 3a), the 'saturated' compound **2** cannot reach the amino acid Trp84 of the anionic center which easily explains the decrease in inhibitory potency (see Fig. 3b). In addition the interaction between the piperidine ring and the Phe331 is not strong. Interestingly, compound **4** which is shorter can find all interaction partner of the AChE mentioned for **1** (see Fig. 3c). Since **4** is less basic it is less positively charged at pH 7.4 which results in a less strong π–cation interaction with Phe331 and, thus, explains the decrease in activity. Compound **5d** makes nice interactions with Trp84 and Tyr334, instead of Phe331, but does not reach the peripheral Trp279, because the phenyl ring points to the wrong direction (see Fig. 3d). This explains the fact that the compound does not have the high inhibitory activity of compound **1**.

2.4. Structure–activity relationships

In contrast to the starting compounds **DUO3** and **1** which are permanently positively charged, the compounds **2**–**5** can be non-protonated according to the pK_a values resulting in a higher lipophilicity (see log *P* values), and, thus, being able to pass the BBB. The neutral form can be regarded as a (membrane) transport form. Additionally, the compounds perfectly fulfill the Lipinski's rule of five[41] and do have less than three hydrogen-bond donors and six

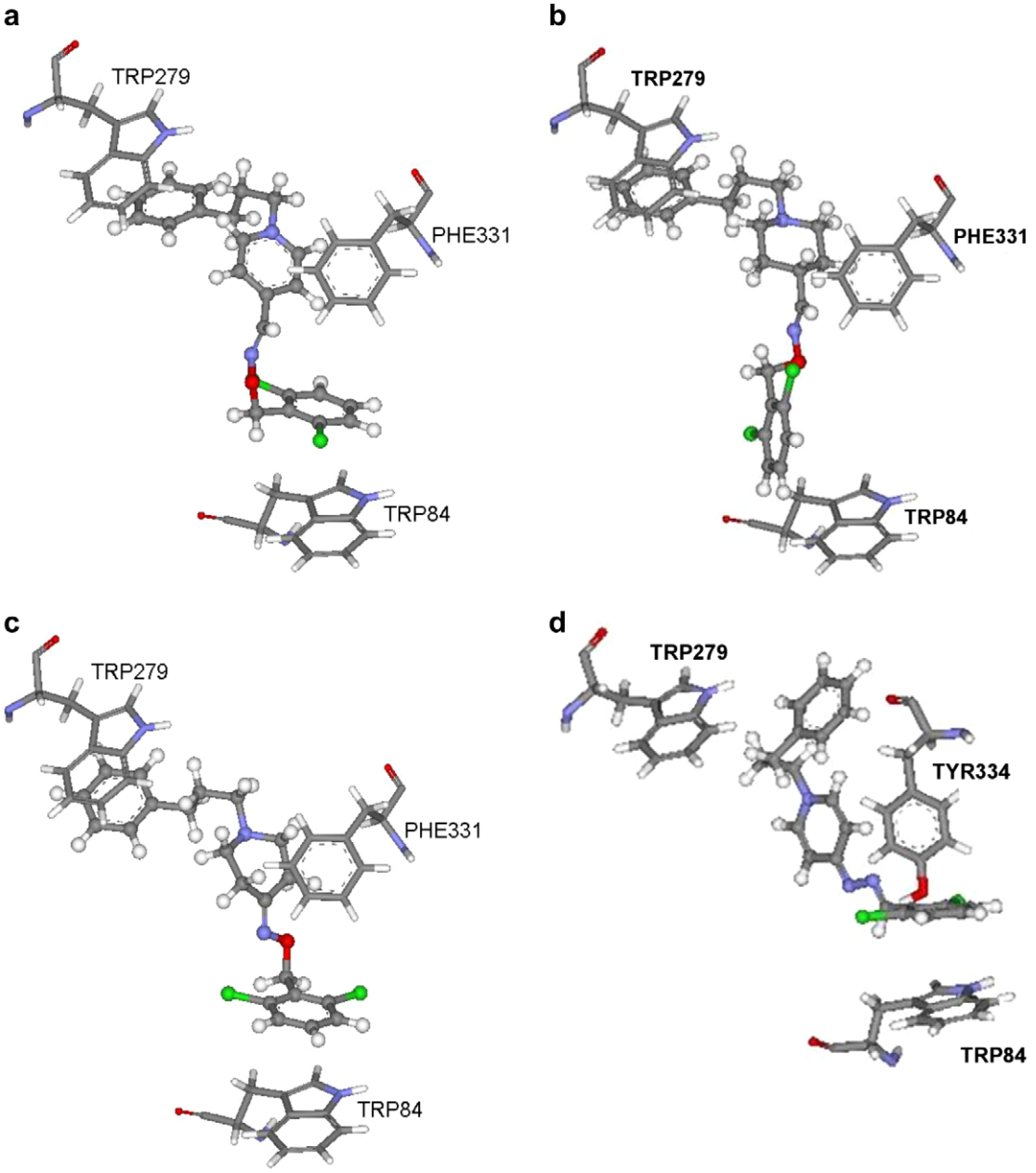

Figure 3. (a) Binding mode of compound **1**, (b) of compound **2**, (c) of compound **4** and (d) of compound **5d**.

hydrogen-bond acceptors which is a special requirement for crossing the BBB.[42] Since they are also ionizable at physiological pH they are theoretically able to form a favorable π–cation interaction with the phenylalanine 331 of the AChE. Taken together, compounds **2–5** fulfill the requirement of being active in the brain which is a step forward compared with **DUO3** and compound **1**.

With exception of compounds **3** and **5a** all compounds are reasonable able to inhibit the AChE activity indicating that the dichlorobenzyl moiety at the oxime end of the molecule and the phenylalkyl skeleton at the 1,4-dihydropyridine nitrogen are belonging to the pharmacophore for AChE inhibition. A series of (benzylidene-hydrazono)-1,4-dihydropyridines compounds having a *p*-chlorobenzyl instead of a 2,6-dichlorobenzyl ring shows analogous inhibitory activities (data not shown).

In order to occupy the active site of the AChE properly, that is, to form a π–π interaction with Trp84 at the bottom of the active site and to reach the peripheral site for π–π interaction with Trp279, a phenylpropyl substituent attached to the piperidine nitrogen, being present in **4** and **5d**, is necessary at least. However, the 'saturated' pyridinium ring, that is, a piperidine ring, cannot properly interact with Phe331 which explains the loss in inhibitory activity of compounds **2** and **4** (Fig. 3b and c). The dihydropyridine moiety in **5d** forms a perfect π–π interaction with Tyr334 (Fig. 3d) which could be expected from the π–π interaction of the dichlorophenyl ring and the 1,4-dihydropyridine observed in crystals (see Fig. 1). In the case of protonation (pK_a 9) at physiological pH a π–cation interaction with Trp334 can be additionally formed.

The docking poses for the **5**-series (shown in Fig. 4) reveal a good correlation between the alkyl chain length (between the dihydropyridine and the phenyl moiety) and the inhibition of AChE with exception of **5e**: the terminal dichlorobenzyl moiety strongly favors an π–π interaction with Trp84, and the constant part of the structure fits reasonably well along the binding pocket. Compound **5d** is the only one that reaches the Trp279 and through its phenyl terminus is able to have a π–π interaction with this tryptophane. The alkyl chain length of **5d** can be seen as almost perfect for the binding pocket of AChE. Strikingly, compound **5e**, which is considerably shorter still exhibits almost the same strength of inhibition. A detailed investigation of its preferred docking pose shows a very interesting result: due to its two dichlorobenzyl moieties this compound fits into the binding pocket exactly the other way round (analogous to the non-**5** compounds). The moiety that interacts with Trp84 in all other cases now interacts with Trp279, whereas the newly introduced dichlorobenzyl is directed towards the inner part of the binding pocket.

In summary, the docking gives a very good interpretation of the activity seen in the experiments and will guide future research. In order to enhance the inhibitory properties of the pyridinylidene hydrazones **5** the future developments have to focus at the optimization of the linkers between the dihydropyridine and both lateral phenyl rings.

Compounds **5c** and **5d**, carrying a phenylpropyl and a phenylethyl residue, were found to be the best inhibitors of the fibril formation even better than **DUO3** whereas compounds **5b** and **5e**, having both a benzyl moiety attached to the 1,4-dihydropyridine nitrogen, are less active. The already formed fibrils can be destroyed by compounds **5b–e** to the same extent. Since **5a** did not show any activity, the second phenyl rings seems to be essential for the inhibition of the fibril formation. Additionally the distance between the dihydropyridine nitrogen and the phenyl rings has to be at least two methylene groups which goes in parallel with the SAR of the AChE inhibitory activity.

3. Conclusion

Starting from the permanently positively charged lead compound **DUO3** which is able to inhibit the activity of the AChE and BuChE as well as the fibril formation of Aβ40, but cannot pass the BBB, we have developed a concept to combine the ability to cross the BBB, to interact with the AChE and BuChE in positively charged form, and even more important to inhibit the plaque formation responsible for the appearance of Alzheimer's disease, and additionally to destroy the already formed plaques. The most active (benzylidene-hydrazono)-1,4-dihydropyridines **5d** merges the inhibition of both the AChE/BuChE and the fibril formation as well as the destruction. In the next step, the inhibitory activities have to be enhanced by variations of the linkers and the substitution pattern. This work is in progress.

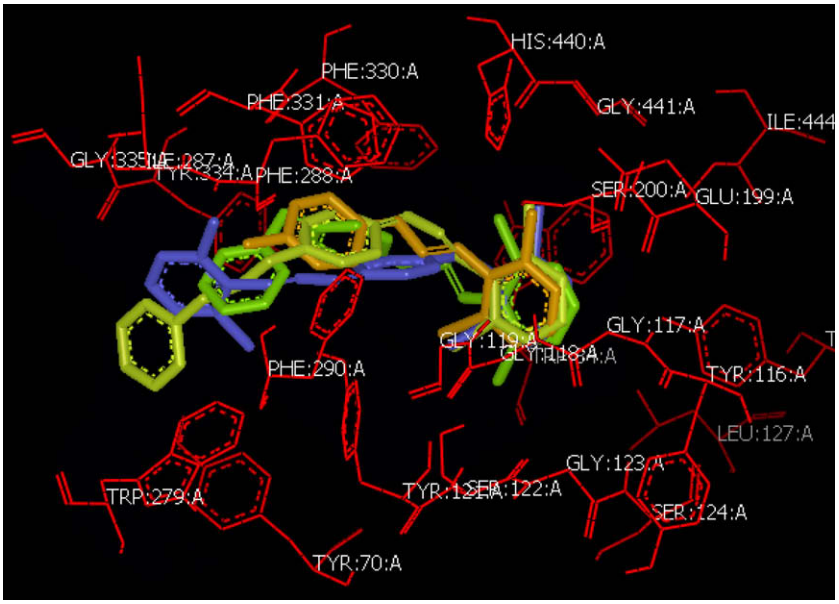

Figure 4. Here the overlay of all 5-series compounds is shown. This figure outlines the interpretation which nicely fits the chain length of the different molecules to its inhibitory activity against AChE with **5e** being an exception (colors: blue **5e**, yellow **5d**, green **5b**, orange **5c**, **5a** is hidden within the orange).

4. Experimental section

4.1. Material and methods

Melting points were determined with a Büchi 510 melting point apparatus (Büchi, Switzerland) and are not corrected. ^{1}H and ^{13}C NMR spectra were recorded on a Bruker AV 400 instrument (^{1}H 400.132 MHz; ^{13}C 100.613 MHz). Abbreviations for data quoted are: s, singlet; d, doublet; t, triplet; quin, quintet; dd, doublet of doublets; m, multiplet; br s, broad signal. The centers of the peaks of $CDCl_3$ and CH_3OH-d_4 were used as internal references (^{1}H NMR $CDCl_3$: 7.26 ppm; CH_3OH-d_4: 3.31; ^{13}C NMR $CDCl_3$: 77.00 ppm; CH_3OH-d_4: 49.00 ppm). IR spectra of compounds were recorded as potassium bromide pellets on a Jasco FT/IR-400 spectrometer. Dry solvents were used throughout. The electron impact (EI) mass spectra were measured on Finnigan Mat 8200. Reagents used for synthesis were purchased from Aldrich, Fluka, and Merck companies. Organic solvents were purchased from Merck Company. Thin-layer chromatographies were done on pre-coated Silica Gel 60 F_{254} plates (Merck). The spots were visualized with UV light or iodine. Microanalyses (C, H, N) of new compounds agreed with the theoretical value within ±0.4%.

The compounds 4-[(2,6-dichlorobenzyloxyimino)methyl]-1-(3-phenylpropyl)-piperidinium hydrochloride (**2**), 1-(3-phenylpropyl)-4-piperidone oxime (**3**), and 1-(2-phenylpropyl)piperidin-4-one *O*-(2,6-dichlorobenzyl)-oxime (**4**) were prepared as described in Ref. 27.

4.2. Synthesis of 4-(2-(2,6-dichlorobenzylidene)hydrazinyl)-pyridine 6

To a solution of 2 g (13.7 mmol) 4-hydrazinylpyridine hydrochloride in EtOH/H_2O (30 ml; 1:1) and 2% triethylamine a solution of 2.5 g (14.3 mmol) 2,6-dichlorbenzaldehyde in EtOH (10 ml) was added. The reaction mixture was refluxed for 12 h, evaporated and the residues purified by chromatography (silica gel, EtOH/H_2O 1:1 with 2% triethylamine). Yield: 2.7 g (76%) of a light yellow solid (mp 242 °C); IR (ATR) *ν* 769, 991, 1120, 1209, 1315, 1421, 1550, 2028, 2159, 2832; ^{1}H NMR (DMSO-d_6): *δ* ppm 6.96 (2H, d, *J* = 6.9 Hz, pyr N–CH–CH), 7.37 (1H, dd, *J* = 8.5/7.7, Ph), 7.5 (2H, d, *J* = 8.1, Ph), 8.21 (1H, s, N=CH), 8.25 (2H, d, *J* = 6.3, pyr N–CH), 11.12 (1H, s, NH).

^{13}C NMR (DMSO-d_6): 107.25 (pyr N–C–C), 129.52 (Ph), 130.13 (Ph), 130.20 (Ph Cl–C–C), 133.50 (Ph C–Cl), 134.97 (N=C), 150.15 (pyr N–C), 150.36 (pyr N–C–C–C).

4.3. General procedure for the synthesis of the 1-substituted (benzylidene-hydrazono)-1,4-dihydropyridines derivatives

1-Substituted 4(1*H*)-pyridinone hydrazones derivatives were synthesized in analogy to Douglas et al.[28] All compounds were recrystallized from methanol, ethanol–water or methanol–water mixture.

4.3.1. 1-Methyl-4-[(2,6-dichlorobenzylidene)hydrazono]-1,4-dihydropyridine 5a

Yield 88%; mp 123 °C; IR (KBr) *ν* 1644, 1493, 1381, 1197, 833, 774 cm^{-1}; ^{1}H NMR (CH_3OH-d_4): *δ* ppm 3.64 (3H, s, *N*–CH_3), 6.40 (1H, dd, *J* = 3.0/7.7 Hz), 7.22 (1H, dd, *J* = 3.0/8.0 Hz), 7.28 (1H, dd, *J* = 7.8/8.6 Hz), 7.35–7.39 (2H, m), 7.45 (2H, d, *J* = 8.0 Hz), 8.50 (1H, s, N=CH); 13C NMR (CH_3OH-d_4): *δ* ppm 43.21 (q), 108.28 (d), 112.01 (d), 130.16 (d), 130.39 (d), 132.96 (s), 135.74 (s), 140.37 (d), 140.84 (d), 145.15 (d), 163.07 (s). EI-MS *m/z* (% relative intensity): 281 (M+2), 279 (M+, 10), 244 (100), 181 (25), 93 (60), 92 (27), 66 (32), 42 (24). Anal. Calcd for ($C_{13}H_{11}N_3Cl_2 \times H_2O$; 298.17 g/mol): C, 52.4; H, 4.39; N, 14.1. Found: C, 52.6; H, 3.99; N, 14.1.

4.3.2. 1-Benzyl-4-[(2,6-dichlorobenzylidene)hydrazono)]-1,4-dihydropyridine 5b

Yield 62%; yellowish oil; IR (KBr) *ν* 1644, 1510, 1393, 1174, 825, 774 cm^{-1}; ^{1}H NMR (CH_3OH-d_4): *δ* ppm 5.01 (2H, s, CH_2-Ph), 6.39 (1H, dd, *J* = 2.5/7.5 Hz,), 7.19–7.46 (11H, m), 8.50 (1H, s, N=CH); 13C NMR (CH_3OH-d_4): *δ* ppm 60.33 (t), 108.54 (d), 112.30 (d), 128.73 (d), 129.60 (d), 130.20 (d), 130.24 (d), 130.56 (d), 132.96 (s), 135.86 (s), 137.61 (s), 139.82 (d), 140.31 (d), 145.73 (d), 163.12 (s). EI-MS *m/z* (% relative intensity): 357 (M+2), 355 (M+), 154 (34), 152 (100), 125 (26), 91 (40), 92 (40), 63 (28). Anal. Calcd for ($C_{19}H_{15}N_3Cl_2$; 356.25 g/mol): C, 64.1; H, 4.23; N, 11.8. Found: C, 63.9; H, 4.56; N, 11.5.

4.3.3. 1-(Phenethyl)-4-[(2,6-dichlorobenzylidene)hydrazono)]-1,4-dihydropyridine 5c

Yield 55%; mp 145 °C; IR (KBr) *ν* 1636, 1484, 1390, 1182, 826, 753 cm^{-1}; ^{1}H NMR (CH_3OH-d_4): *δ* ppm 3.04 (2H, t, *J* = 6.8 Hz, CH_2), 4.06 (2H, t, *J* = 6.9 Hz, CH_2), 6.29 (1H, dd, *J* = 2.7/7.7 Hz), 7.11 (1H, dd, *J* = 2.7/7.4 Hz), 7.17 (1H, dd, *J* = 1.5/8.3 Hz), 7.22–7.30 (7H, m), 7.42 (2H, d, *J* = 8.3 Hz), 8.51 (1H, s, N=CH); 13C NMR (CH_3OH-d_4): *δ* ppm 38.04 (t), 58.73 (t), 108.21 (d), 111.84 (d), 128.00 (d), 129.81 (d), 130.04 (d), 130.25 (d), 130.49 (d), 132.96 (s), 135.81 (s), 138.55 (s), 139.75 (d), 140.18 (d), 145.33 (d), 163.16 (s); EI-MS *m/z* (% relative intensity): 371 (M+2), 369 (M+), 334 (24), 105 (100), 79 (20). Anal. Calcd for ($C_{20}H_{17}N_3Cl_2$; 370.28 g/mol): C, 64.9; H, 4.63; N, 11.4. Found: C, 64.7; H, 4.78; N, 11.2.

4.3.4. 1-(3-Phenylpropyl)-4-[(2,6-dichlorobenzylidene)hydrazono)]-1,4-dihydropyridine 5d

Yield 52%; yellowish oil; IR (KBr) *ν* 1644, 1509, 1393, 1186, 825, 774 cm^{-1}; ^{1}H NMR (CH_3OH-d_4): *δ* ppm 2.12 (2H, quin, *J* = 7.3 Hz, CH_2), 2.68 (2H, t, *J* = 7.4 Hz, CH_2), 3.86 (2H, t, *J* = 7.3 Hz, CH_2), 6.42 (1H, d, *J* = 6.3 Hz,), 7.18–7.33 (7H, m), 7.39–7.48 (4H, m), 8.52 (1H, s, N=CH); 13C NMR (CH_3OH-d_4): *δ* ppm 33.38 (t), 54.90 (t), 56.86 (t), 108.45 (d), 112.15 (d), 127.27 (d), 129.41 (d), 129.64 (d), 130.25 (d), 130.51 (d), 132.99 (s), 135.83 (s), 139.69 (d), 140.17 (d), 141.96 (s), 145.33 (d), 163.21 (s); EI-MS *m/z* (% relative intensity): 385 (M+2), 383 (M+), 348 (24), 230 (11), 91 (100), 79 (11), 51 (11), 41 (11). Anal. Calcd for ($C_{21}H_{19}N_3Cl_2$; 384.31): C, 65.6; H, 4.98; N, 11.9. Found: C, 65.6; H, 5.22; N, 10.8.

4.3.5. 1-(2,6-Dichlorobenzyl)-4-[(2,6-dichlorobenzylidene)hydrazono)]-1,4-dihydropyridine 5e

Yield 74%; yellowish oil; mp 204 °C; IR (KBr) *ν* 1640, 1486, 1436, 1170, 825, 780 cm^{-1}; ^{1}H NMR ($CDCl_3$): *δ* ppm 5.14 (2H, s, *CH$_2$-Ph*), 6.53 (1H, br s), 7.08–7.33 (8H, m), 7.42 (2H, d, *J* = 8.6 Hz), 8.69 (1H, s, N=CH); 13C NMR ($CDCl_3$): *δ* ppm 53.82 (t), 107.85 (d), 112.31 (d), 128.81 (d), 128.95 (d), 129.17 (d), 130.16 (s), 131.02 (d), 135.03 (s), 136.71 (s), 137.56 (s), 138.62 (d), 141.15 (d), 146.49 (d), 163.05 (s); EI-MS *m/z* (% relative intensity): 425 (M+2), 421 (M+1), 423 (M+), 159 (100), 123 (15), 51 (15), 49 (35). Anal. Calcd for ($C_{19}H_{13}N_3Cl_4$; 425.14): C, 53.7; H, 3.08; N, 9.9. Found: C, 53.9; H, 3.23; N, 9.7.

4.4. pK_a determination

The experimental determination of the pK_a values was performed on a Sirius PCA-101 (Sirius Analytical Instruments Ltd, Forest Row, East Sussex, United Kingdom). The compounds were dissolved in 0.15 M KCl to keep the ionic strength constant during titration. 30% Dioxane (compounds **2** and **4**) and 80% methanol (**5d**) were used as modifier for complete dissolution. The pH was adjusted to 1.8 by adding 0.5 M HCl. With 0.5 M KOH titration was performed. The dissociation constant calculated by the program PKALOGP5.1 (Sirius Analytical Instruments Ltd) was determined

for different additions of the modifier. The pK_a values were obtained by extrapolation of the calibration line. In order to calibrate the electrode, blank titrations were performed, titrating the 0.15 M KCl solution and determining the corresponding 'Four Plus™'-parameters.

4.5. Log *P* determination

4.5.1. Log *P* determination by means of RP HPLC

The partition coefficients of all compounds were determined by RP-chromatography using methanol/phosphate buffer 70/30 as an eluent. The chromatographic systems were calibrated with solutes for which an experimental octanol/water partition coefficient was available.[43] The capacity factors of the reference substances were correlated against with experimental octanol/water log *P* values, and the obtained correlation equation was used to calculate log *P* values of the tested compounds. The experiments were performed on a LiChroCART® 125–4.6 HPLC-Cartridge filled with LiChrospher® 100, RP18, 5 μm, endcapped (Merck, Darmstadt, Germany). The methanol (LiChrosolv® (Merck))/buffer (70/30) mobile phase was used at a flow-rate of 1.0 ml. The phosphate buffer (pH 7.4, DAB 1999) was obtained by mixing a 0.2 M potassium dihydrogen phosphate solution (1000 ml) and 0.1 M sodium hydroxide (1573 ml). 0.02% *N*,*N*-Dimethylhexylamine was added to minimize the peak tailing.

The following aromatic compounds were applied for calibration: 2-phenylethanol, benzene, dimethylaniline, toluene, biphenyl, anthracene.

The analytes were dissolved in methanol at a concentration of 4 μg/ml. Experiments were run in duplicate, and peak maxima were determined at the respective absorption maximum. Capacity ratios were determined as $k' = (t_r - t_o)/t_o$, where t_r is the average retention time of the analyte and t_o is the average retention time of the solvent. A linear regression was performed for the log k'/log *P* data of the reference compounds ($y = 2.5935 + 1.8353$; $r^2 = 0.9782$), and the regression equation was used to calculate the log *P* of the compounds.

4.5.2. Log *P* determination by means of shake flask method

Partition coefficients of **5d** and **5e** were determined by shake flask method using UV spectroscopy and were studied in phosphate buffer at pH 5, 6, 7, and 7.4 for each compound. The phosphate buffer was saturated with octanol prior to partitioning by adding octanol, mixing, and allowing the phases to separate overnight; in the same manner portions of octanol were saturated with the buffer. A stock solution for each compound was prepared at 10^{-5} mol/l concentration in octanol saturated with phosphate buffer and the absorbance (A_o) was measured between 314 and360 nm. A 1.0 ml portion of this solution was shaken at 37 °C for 4 h with 1.0 ml phosphate buffer saturated with octanol. The emulsion was allowed to stand overnight, centrifuged for 5 min (3000 U/min), the water layer separated and again the absorption (A_1) measured and the log *P* value was calculated as $\log P = \log((A_o - A_1)/A_1)$.

4.6. Crystal structure determination

The crystal data of **5a** were collected at Bruker X8Apex diffractometer with CCD area detector and multi-layer mirror monochromated Mo Kα radiation. The structure was solved using direct methods, refine with SHELX software package (G. Sheldrick, University of Göttingen 1997) and expanded using Fourier techniques. All non-hydrogen atoms were refined anisotropically. Hydrogen atoms were assigned idealized positions and were included in structure factors calculations.

Crystal data for **5a**: $C_{13}H_{11}Cl_2N_3 \times H_2O$, $M_r = 280.15644$ ($C_{13}H_{11}Cl_2N_3$) + 18.01528 (H_2O) = 298.17172, yellow needle, 0.20×0.10×0.06, monoclinic space group $P2_1/n$, $a = 13.9396(3)$, $b = 7.0876(2)$, $c = 14.3087(3)$ Å, $\beta = 107.4800(10)°$, $V_c = 1348.39(6)$ Å^3, $Z = 4$, $\rho_{calcd} = 1.469$ g cm^{-3}, $\mu = 0.476$ mm^{-1}, $F(0\,0\,0) = 616$, $T = 100(2)$ K, $R_1 = 0.0389$, $wR^2 = 0.0953$, 4124 independent reflections [$2\theta \leqslant 64°$] and 178 parameters.

Crystallographic data have been deposited with the Cambridge Crystallographic Data Center as supplementary publication no. CCDC-709897. These data can be obtained free of charge from The Cambridge Crystallographic Data Centre via www.ccdc.cam.ac.uk/data_request/cif.

4.7. Inhibition of AChE

The inhibitory potency against AChE was investigated by slightly modified colorimetric method of Ellman et al.[44] as reported in Ref. 48. Acetylcholinesterase (AChE) –E.C. 3.1.1.7 from Electric Eel was purchased from Sigma–Aldrich (Steinheim, Germany). 5,5′-Dithiobis-(2-nitrobenzoic acid), potassium dihydrogen phosphate, potassium hydroxide, sodium hydrogen carbonate, and acetylthiocholine iodide were obtained from Fluka (Buchs, Switzerland). Spectrophotometric measurements were performed on a Varian Cary 50 UV–vis spectrophotometer. Details of the inhibition study are given in Kapková et al.[22]

4.8. Inhibition of BuChE

BuChE inhibitory activity was investigated by a modified Ellman's test, conducted as in Ingkaninan et al.[45] Details of the method using the BuChE (EC 3.1.1.8, from horse serum) are given in Fallarero et al.[7]

4.9. Thioflavin T Fluorescence Assay (all carried out in analogy to[46,47])

4.9.1. Aβ

Amyloid β-protein (1–40) trifluoroacetate salt was obtained from Bachem (Switzerland, Lot 1012093; Lot 9004754). The peptide was stored at −20 °C, as recommended by the manufacturer. It was dissolved in hexafluoroisopropanol (HFIP) at 20 mg/ml. This solution was kept at room temperature until the peptide was completely dissolved (30 min to 1 h). The HFIP was removed under a stream of nitrogen until a clear film remained in the test tube. The residue was then dissolved in DMSO to obtain a 2 mM stock solution, which was subsequently stored frozen at −20 °C for maximum three days.

4.9.2. ThT assay Aβ

A 2 mM stock solution of Aβ in DMSO was diluted in buffer (25 mM NaH_2PO_4, 120 mM NaCl, 3 μM thioflavin T, 0.02% NaN_3 and a final pH of 7.4) to reach a final peptide concentration of 100 μM. Inhibitors were added to reach concentrations between 0.005 and 0.5 mM. Incubations were performed at 37 °C on 96-well fluorescence microtiter plates (Nunc GmbH, Wiesbaden, Germany). The fluorescence was measured (excitation wavelength 450 nm, emission wavelength 482 nm) on a Cary Eclipse fluorescence spectrophotometer (Varian, Darmstadt, Germany).

4.9.3. ThT assay fibril formation with peptide HHQKLVFFAED

Inhibitors were diluted in buffer (25 mM NaH_2PO_4, 120 mM NaCl, 3 μM thioflavin T, 0.02% NaN_3 and a final pH of 7.4) to reach concentrations between 0.005 and 0.5 mM. A 2 mM stock solution of the peptide HHQKLVFFAED in DMSO was added to reach a final peptide concentration of 100 μM. Incubations were performed on 96-well fluorescence microtiter plates (Nunc GmbH, Wiesbaden,

Germany). The fluorescence was measured (excitation wavelength 450 nm, emission wavelength 482 nm) on a Cary Eclipse fluorescence spectrophotometer (Varian, Darmstadt, Germany).

4.9.4. ThT assay fibril destruction with peptide HHQKLVFFAED

A 2 mM stock solution of the peptide HHQKLVFFAED in DMSO was diluted in buffer (25 mM NaH_2PO_4, 120 mM NaCl, 3 μM thioflavin T, 0.02% NaN_3 and a final pH of 7.4) to reach a final peptide concentration of 100 μM. Incubations were performed on 96-well fluorescence microtiter plates (Nunc GmbH, Wiesbaden, Germany) for 10 h. Inhibitors were added to reach concentrations between 0.005 and 0.5 mM. The fluorescence was measured (excitation wavelength 450 nm, emission wavelength 482 nm) on a Cary Eclipse fluorescence spectrophotometer (Varian, Darmstadt, Germany).

4.10. Solid phase synthesis of HHQKLVFFAED

The shortened peptide was synthesized by solid-phase peptide synthesis on a Milligen 9050 PepSynthesiser using standard Fmoc protocol.[48] Synthesis was performed in DMF/DCM (60:40) with DIC/HOBt activation starting from Fmoc-Asp(OtBu)-Wang-resin. The peptide was cleaved from the resin by treatment with TFA/H_2O/TIS (95/2.5/2.5). The following side chain protecting groups were used during the automated synthesis: *tert*-butyl ester (Glu), *tert*-butyloxycarbonyl (Lys), and trityl (Gln, His).

The product substrate as TFA salt was purified by HPLC (H_2O + 0.1% TFA; acetonitrile (Merck); LiChroCART® 125–4.6 HPLC-Cartridge (LiChrospher® 100, RP18 (5 μm, endcapped), (Merck); pressure: 143 bar; flow-rate: 1.0 ml; temperature: 23 °C; eluent gradient: acetonitrile/water + 0.1% TFA 20–80% in 40 min. The peptide was stored at −20 °C. For each test a fresh solution of 2 mM in DMSO was prepared.

4.11. Determination of the protonated sites

4.11.1. Conformational search

The conformational search was performed using the MMFF94 force field as implemented in MacroModel 8.0.[49]

4.11.2. Geometry optimization

The DFT calculations were carried out with TURBOMOL 5.6 program package.[37] Full geometry optimizations were performed at the BP86/TZVP level of theory using the RI approximation. Solvation effects were taken into account via the COSMO approach as implemented in TURBOMOL employing an dielectric constant of $\varepsilon = 78$ to simulate a water-like solvent.

4.11.3. pK_a calculation

pK_a determination was performed by COSMO-RS approach implemented in COSMOthermX. Calculating ΔG_{diss} of the protonated molecule by TZVP the corresponding pK_a values were determined.

4.12. Docking

The structures carrying protonation state information determined in the first step where exported with their connection tables to a format readable by Openeye Omega. Precalculated coordinates were not used for the subsequent steps as the applied docking algorithm requires a set of conformers for each molecule that is docked. This set of possible conformers for each compound was generated using Omega's standard procedure with the option '-fromCT'. Further constraints were not used in this step. The hereby generated conformers were then docked into the crystal structure of *T. californica* AChE (PDB: 1EVE). This structure was chosen because of its previous successful use in similar experiments.[22] The protein structure was prepared as follows: The co-crystallized ligand (1-benzyl-4-[(5,6-dimethoxy-1-indanon-2-yl)methyl]piperidine) in EVE was used as a starting point. All amino acids where at least one atom has a distance of not more than 6 Å to the original ligand were selected for the binding pocket definition. This reduced protein structure information was then exported in the native Openeye format. Next, the binding pocket was read into Openeye Fred. Every conformer of every ligand was docked into this pre-defined binding pocket by using Fred's standard parameters. Beside the binding pocket no constraints were applied. The best pose for each compound was then used by applying all scoring functions available in FRED to obtain a consensus score for a ranking of the docked conformers. This scoring was only applied within conformer sets, but not for the qualitative analysis of binding modes. Only the analysis of this top-ranking result in the crystal structure was then analyzed in depth and the result was interpreted.

Acknowledgements

The authors thank the TUBITAK-DFG for a grant given to V.A. and the Fonds der Chemischen Industrie for financial support. U.H. and B.E. thank the SFB630 for financial support. Thanks are due to Professor Schirmeister for helping with the peptide synthesis and providing the synthesizer. J.S. thanks Markus Kossner/TU Braunschweig for fruitful discussions about the use of Openeye FRED.

References and notes

1. Rajkumar, S.; Tanyakitpisal, P.; Chandra, V. WHO, 2001.
2. Jakob-Roetne, R.; Jacobsen, H. *Angew. Chem.* **2009**, *121*, 3074.
3. Roberson, E. D.; Mucke, L. *Science* **2006**, *314*, 781.
4. Davies, P.; Maloney, A. J. *Lancet* **1976**, *2*, 1403.
5. Bartus, R. T.; Dean, R. L., III; Beer, B.; Lippa, A. S. *Science* **1982**, *217*, 408.
6. Holzgrabe, U.; Kapkova, P.; Alptüzün, V.; Scheiber, J.; Kugelmann, E. *Expert Opin. Ther. Targets* **2007**, *11*, 161.
7. Fallarero, A.; Oinonen, P.; Gupta, S.; Blom, P.; Galkin, A. *Pharmacol. Res.* **2008**, *58*, 215.
8. Decker, M.; Kraus, B.; Heilmann, J. *Bioorg. Med. Chem.* **2008**, *16*, 4252.
9. Kamal, M. A.; Klein, P.; Luo, W.; Li, Y.; Holloway, H. W.; Tweedie, D.; Greig, N. H. *Neurochem. Res.* **2008**, *33*, 745.
10. Doody, R. S.; Gavrilova, S. I.; Thomas, R. G.; Aisen, P. S.; Bachurin, S. O.; Seely, L.; Hung, D. *Lancet* **2008**, *372*, 207.
11. Hamley, I. W. *Angew. Chem., Int. Ed.* **2007**, *46*, 8128.
12. Olsen, R. E.; Marcin, L. R. *Annu. Rep. Med. Chem.* **2007**, *42*, 27.
13. Austen, B. M.; Paleologou, K. E.; Ali, S. A. E.; Qureshi, M. M.; Allsop, D.; El-Agnaf *Biochemistry* **2008**, *47*, 1984.
14. Török, B.; Dasgupta, S.; Török, M. *Curr. Bioactive Comp.* **2008**, *4*, 159.
15. Recanatini, M.; Valenti, P. *Curr. Pharm. Des.* **2004**, *10*, 3157.
16. Piazzi, L.; Rampa, A.; Bisi, A.; Gobbi, S.; Belutti, F.; Cavalli, A.; Bartolini, M.; Andrisano, V.; Valenti, P.; Recanatini, M. *J. Med. Chem.* **2003**, *46*, 2279.
17. Cavalli, A.; Bolognesi, M. L.; Minarini, A.; Rosini, M.; Tumiatti, V.; Recanatini, M.; Melchiorre, C. *J. Med. Chem.* **2008**, *51*, 347.
18. Hardy, J. *J. Neurochem.* **2009**, *110*, 1129.
19. Greig, N. H.; Sambamurti, K.; Yu, Q. S.; Brossi, A.; Bruinsma, G. B.; Lahiri, D. K. *Curr. Alzheimer Res.* **2005**, *2*, 281.
20. Rizzo, S.; Rivière, C.; Piazzi, L.; Bisi, A.; Gobbi, S.; Bartolini, M.; Andrisano, V.; Morroni, F.; Tarozzi, A.; Monti, J. P.; Rampa, A. *J. Med. Chem.* **2008**, *51*, 2883.
21. Camps, P.; Formosa, X.; Galdeano, C.; Gómez, T.; Muñoz-Torrero, D.; Scarpellini, M.; Viayna, E.; Badia, A.; Clos, M. V.; Camins, A.; Pallàs, M.; Bartolini, M.; Mancini, F.; Andrisano, V.; Estelrich, J.; Lizondo, M.; Bidon-Chanal, A.; Luque, F. J. *J. Med. Chem.* **2008**, *51*, 3588.
22. Kapková, P.; Stiefl, N.; Sürig, U.; Engels, B.; Baumann, K.; Holzgrabe, U. *Arch. Pharm. (Weinheim)* **2003**, *336*, 523.
23. Alptüzün, V.; Kapková, P.; Baumann, K.; Erciyas, E.; Holzgrabe, U. *J. Pharm. Pharmacol.* **2003**, *10*, 1397.
24. Kapková, P.; Alptüzün, V.; Frey, P.; Erciyas, E.; Holzgrabe, U. *Bioorg. Med. Chem.* **2006**, *14*, 472.
25. Bodor, N.; Buchwald, P. *Drug Discovery Today* **2002**, *7*, 766.
26. Shoval, H.; Lichtenberg, D.; Gazit, E. *Amyloid* **2007**, *14*, 73.
27. Goebel, T.; Ulmer, D.; Projahn, H.; Ponte-Sucre, A.; Saeftel, M.; Hoerauf, A.; Kaiser, A.; Hauber, I.; Hauber, J.; Holzgrabe, U. *J. Med. Chem.* **2008**, *51*, 238.
28. Douglas, W. A.; Fishinger, J. J.; Gund, P.; Haris, E. E.; Olson, G.; Patchett, A. A.; Ruyle, W. V. *J. Med. Chem.* **1977**, *20*, 939.
29. Avdeef, A.; Box, K. J.; Comer, J. E. A.; Gilges, M.; Hadley, M.; Hibbert, C.; Patterson, W.; Tam, K. Y. *J. Pharm. Biomed. Anal.* **1999**, *20*, 631.

30. Van der Waterbeemd, H.; Kansy, M.; Wagner, B.; Fischer, H. In *Lipophilicity in Drug Action and Toxicology*; Pliska, V., Testa, B., Van der Waterbeemd, H., Eds.; Series: Methods and Principles in Medicinal Chemistry; VCH, 1996; Vol. 4, p 89.
31. Gazit, E. *FEBS J.* **2005**, *272*, 5971.
32. De Felice, F. G.; Vieira, M. N. N.; Saraiva, L. M.; Figueroa-Villar, J. D.; Garcia-Abreu, J.; Liu, R.; Chang, L.; Klein, W. L.; Ferreira, S. T. *FASEB J.* **2004**, *18*, 1366.
33. Camus, M. S.; Dos Santos, S.; Chandravarkar, A.; Mandal, B.; Schmid, A. W.; Tuchscherer, G.; Mutter, M.; Lashuel, H. A. *ChemBioChem* **2008**, *9*, 2104.
34. Coupez, B.; Lewis, R. A. *Curr. Med. Chem.* **2006**, *13*, 2995.
35. Halgren, T. A. *J. Comput. Chem.* **1996**, *17*, 490–641.
36. Klamt, A.; Schüürmann, G. *J. Chem. Soc., Perkin Trans. 2* **1993**, 799.
37. Schäfer, A.; Klamt, A.; Sattel, D.; Lohrenz, J. C. W.; Eckert, F. *Phys. Chem. Chem. Phys.* **2000**, *2*, 2187.
38. Becke, A. D. *Phys. Rev. A* **1988**, *38*, 3098.
39. Eichkorn, K.; Treutler, O.; Öhm, H.; Häser, M.; Ahlrichs, R. *Chem. Phys. Lett.* **1995**, *240*, 283.
40. Klamt, A. *J. Phys. Chem.* **1995**, *99*, 2224.
41. Lipinski, C. A.; Lombardo, F.; Dominy, B. W.; Feeney, P. J. *Adv. Drug Delivery Rev.* **2001**, *46*, 3.
42. Silverman, R. B. *The Organic Chemistry of Drug Design and Drug Action*, 2nd ed.; Elsevier: Amsterdam, 2004. p 66.
43. Hansch, C.; Sammer, P. G.; Taylor, J. B. *Comprehensive Medicinal Chemistry*, 1st ed., Pergamon Press: Oxford; 1990; Vol. 6.
44. Ellman, G. L.; Courtney, D. K.; Andres, V.; Feather-Stone, R. M. *Biochem. Pharmacol.* **1961**, *7*, 88.
45. Ingkaninan, K.; de Best, C. M.; van der Heijden, R.; Hofte, H. J.; Karabatak, B.; Irth, H.; Tjaden, U. R.; van der Greef, J.; Verpoorte, R. *J. Chromatogr., A* **2000**, *872*, 61.
46. Goldsbury, C. S.; Wirtz, S.; Müller, S. A.; Sunderji, S.; Wicki, P.; Aebi, U.; Frey, P. *J. Struct. Biol.* **2000**, *130*, 217.
47. LeVine, H. *Protein Sci.* **1993**, *2*, 404.
48. Bodanszky, M. *Principles of Peptide Synthesis*; Springer: Berlin, Heidelberg, 1993.
49. Mohamadi, F.; Richards, N. G. J.; Guida, W. C.; Liskamp, R.; Lipton, M.; Caufield, C.; Chang, G.; Hendrickson, T.; Still, W. C. *J. Comput. Chem.* **1990**, *11*, 440.
50. Botero Cid, M. H.; Holzgrabe, U.; Kostenis, E.; Mohr, K.; Tränkle, C. *J. Med. Chem.* **1994**, *37*, 1439.